



# Spatial and vertical variability of primary production in the Kara Sea in July and August 2016: the influence of the river plume and subsurface chlorophyll maxima

A. B. Demidov<sup>1</sup> · V. I. Gagarin<sup>1</sup> · O. V. Vorobieva<sup>2,3</sup> · P. N. Makkaveev<sup>1</sup> · V. A. Artemiev<sup>1</sup> · A. N. Khrapko<sup>1</sup> · A. V. Grigoriev<sup>1</sup> · S. V. Sheberstov<sup>1</sup>

Received: 19 April 2017 / Revised: 9 October 2017 / Accepted: 27 November 2017  
© Springer-Verlag GmbH Germany, part of Springer Nature 2017

## Abstract

Seasonal variations in primary production (PP) in the Kara Sea are underresearched. Previous studies only collected data during autumn or in late summer. However, the middle of summer is close to the beginning of the growing season, when PP can contribute significantly to annual water column integrated primary production (IPP). In addition, differences can be expected in the spatial and vertical distribution of phytoplankton communities in this period. This gap in midsummer data was addressed within the framework of a multidisciplinary research cruise by the R/V “Akademik Mstislav Keldysh” (from 15 July to 18 August 2016). High values of IPP ( $> 200 \text{ mgC m}^{-2} \text{ day}^{-1}$ ) and surface chlorophyll *a* (Chl *a*) concentration ( $\text{Chl}_0 > 1 \text{ mg m}^{-3}$ ) were associated with the Ob–Yenisey river plume, located in the central part of the Kara Sea. Beyond the influence of the plume, in the western and southwestern regions of the Kara Sea, well-pronounced subsurface chlorophyll maxima (SCM) were observed. In some cases, the Chl *a* concentration in SCM exceeded  $\text{Chl}_0$  by two orders of magnitude. SCM were often accompanied by subsurface PP maxima (SPM). At stations where SCM was pronounced, IPP values reached  $500\text{--}800 \text{ mgC m}^{-2} \text{ day}^{-1}$ , and  $> 30 \%$  of IPP was accounted for by SPM-integrated PP. Thus, in the middle of summer in the Kara Sea, IPP was linked with the chlorophyll-specific phytoplankton biomass and depended on the strength of the SCM.

**Keywords** Primary production · Chlorophyll · Chlorophyll-specific carbon fixation rate · Kara Sea · Subsurface chlorophyll maximum · River plume

## Introduction

Contemporary decreases in sea ice cover in the Arctic Ocean (Stroeve et al. 2007, 2012a, 2012b; Arrigo et al. 2008; Comiso et al. 2008; Kwok et al. 2009; Zhang et al. 2010; Leu et al. 2011; Cavalieri and Parkinson 2012; Comiso 2012) are especially evident in Siberian seas (Pabi et al. 2008; Arrigo

and van Dijken 2015). Increases in the open water area and duration of the growing season have led to an increase in annual water column integrated primary production (IPP) and influenced the long-term variation of productivity parameters (Arrigo et al. 2008; Pabi et al. 2008; Arrigo and van Dijken 2011; Bélanger et al. 2013; Petrenko et al. 2013; Vancoppenolle et al. 2013).

The Kara Sea is different from most other Arctic seas because of the strong influence of river runoff. Two of the largest rivers discharging into the Arctic Ocean are the Ob and Yenisey with combined average annual runoff of  $981\text{--}1100 \text{ km}^3$  (Gordeev et al. 1996; Holmes et al. 2000, 2012; Dittmar and Kattner 2003; Fütterer and Galimov 2003; Gordeev and Kravchishina 2009), more than 40 % of the total river discharge into the Arctic Ocean (Opsahl et al. 1999). The specific conditions for primary production (PP) are caused by sharp spatial and vertical gradients in environmental factors, high dissolved matter (DOM) and particulate

**Electronic supplementary material** The online version of this article (<https://doi.org/10.1007/s00300-017-2217-x>) contains supplementary material, which is available to authorized users.

✉ A. B. Demidov  
demspa@rambler.ru

<sup>1</sup> Shirshov Institute of Oceanology, Russian Academy of Science, 36 Nakhimovsky av, Moscow, Russia 117997

<sup>2</sup> Lomonosov Moscow State University, Moscow, Russia

<sup>3</sup> Russian Federal Research Institute of Fisheries and Oceanography, Moscow, Russia

organic matter (POM) concentrations, high turbidity, and the limited depth of the euphotic layer.

Despite scientific interest in the Kara Sea, it is an under-sampled region and the contribution of Kara Sea data to the Arctic Ocean PP database remains insufficient (Hill et al. 2013; Matrai et al. 2013; Lee et al. 2015). Therefore, obtaining new experimental data is one of the main tasks of investigations in this region. Field observations throughout the growing season could enable description of the seasonal variability in water column integrated primary production (IPP) values. However, it is often impossible to conduct field explorations because of poor weather conditions and logistical problems over most of the year. Currently, studies of the seasonal variability of IPP in the Kara Sea can only be conducted by using satellite-derived data (Demidov et al. 2017b).

Studies of the Kara Sea PP have been carried out from August to October in different years (Bobrov et al. 1989; Vedernikov et al. 1995; Mosharov 2010; Demidov et al. 2014; Mosharov et al. 2016). However, the growing season, from April to the middle of August, remains unexplored. The ARCSS-PP database (<https://www.nodc.noaa.gov/cgi-bin/OAS/prd/project/details/633>) only contains data from 1998 to 1999 for the St. Anna Trough. Investigations of the spatial and vertical variability of PP characteristics for the rest of the Kara Sea have not been performed. Therefore, results from the period from the second half of July to the middle of August could expand our knowledge of the seasonal dynamics of PP in regions of the Kara Sea beyond the St. Anna Trough.

In recent studies of autumn-season PP, quantitative links were established between the parameters of phytoplankton productivity and biotic and abiotic factors, and the characteristics of the vertical distribution of PP and chlorophyll *a* (Chl *a*) were explored. These studies showed that, in autumn, PP depended mainly on phytoplankton assimilation activity. The high values of surface chlorophyll at the end of the growing season were not an index of water column phytoplankton productivity; production characteristics depended mainly on photosynthetically available radiation (PAR) (Demidov et al. 2014). Also, in autumn, subsurface chlorophyll maximum (SCM) was not a characteristic of the vertical Chl *a* distribution. At the end of the growing season, Chl *a* maxima were, on average, observed at the surface. SCM contributed from 1 to 27 % to water column primary production (Demidov and Mosharov 2015). The novel data provided an opportunity to test the following hypotheses: (1) the impact of PAR and Chl *a* specific biomass on PP in summer and autumn is different, and (2) the influence of SCM on IPP in summer is more significant than in autumn.

The spatial distribution of the Kara Sea PP characteristics largely depends on the spatial variability of river discharge (Demidov et al. 2014). The patterns of PP in regions

influenced by riverine waters and in areas beyond such influence are different. The maximum of river flood occurs in June (Holmes et al. 2012; Le Fouest et al. 2013). Therefore, it is valuable to compare such contrasting areas in the middle of summer when the impact of river discharge is close to maximum.

Thus, the main aims of this study are: (1) to describe the spatial distribution of PP parameters [IPP, Chl *a*, chlorophyll-specific carbon fixation rate ( $P_{opt}^b$ )], and environmental factors in the middle of summer; (2) to investigate the characteristics of the vertical variation of these variables and to estimate the contribution of SCM to IPP in summer; and (3) to compare the results obtained in summer and autumn.

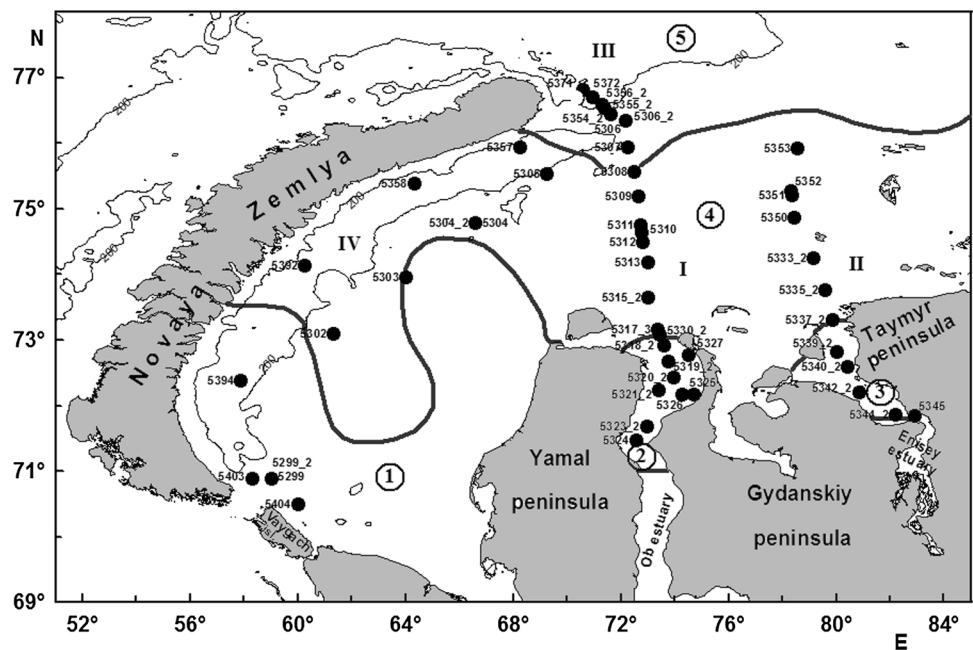
## Materials and methods

### Field data, sampling sites, and Kara Sea subregions

PP parameters for phytoplankton were measured in the open Kara Sea and in the Ob and Yenisey Estuaries during the 66th multidisciplinary research cruise of the R/V “Akademik Mstislav Keldysh” from 15 July to 18 August 2016 (Fig. 1; Online Resource 1). There are hydrological and biogeochemical differences between different regions of the Kara Sea. These differences are caused by changes in the influence of rivers on estuaries and the open sea, and underlie the classification of the Kara Sea water mass (Pivovarov et al. 2003). Based on this classification, we delineated the southwestern subregion (1), the Ob Estuary (2), the Yenisey Estuary (3), the Ob–Yenisey area of river runoff (4), and the northern subregion (5) (area of St. Anna and Voronin Troughs) (Demidov et al. 2014). Subregions 1, 4, and 5 were demarcated using the mean annual surface isohaline of 25 psu (practical salinity units) (Pivovarov et al. 2003). In later studies, the southern boundary of subregion 4 was changed according to the location of a quasistationary desalinated lens in the vicinity of Novaya Zemlya (Zatsepin et al. 2010; Kubryakov et al. 2016).

The Ob and Yenisey Estuaries were considered separately because of previously reported differences in environmental conditions and PP (Vedernikov et al. 1995; Demidov et al. 2014). The mean position of the 10-psu isohaline that was demarcated during earlier Kara Sea expeditions (Vedernikov et al. 1995; Mosharov 2010; Mosharov et al. 2016) was taken as the northern boundary of the estuaries. It is known that average salinity in the range of 2–10 psu is a feature of the Ob and Yenisey Estuaries (Zatsepin et al. 2010; 2017). These areas are known as so-called mixohaline zones (0.5–30 psu), according to the Venice System (Anonymous 1958). Null salinity was used for the southern boundary of the estuaries.

**Fig. 1** Locations of stations in offshore Kara Sea regions, as well as in the Ob and Yenisey Estuaries, which data were gathered during July–August 2016. The sampling sites are denoted as follows: *I*—Ob transect, *II*—Yenisey transect, *III*—transect on the western slope of the St. Anna Trough, *IV*—west and southwest of the Kara Sea. The coordinates of the stations are given in Online Resource 1. Numerals in circles designate hydrological regions of the Kara Sea according to Demidov et al. (2017): 1—southwestern region; 2—Ob Estuary; 3—Yenisey Estuary; 4—river runoff region; 5—northern region



## Sampling procedure

Sampling sites were determined using temperature, salinity, and Chl *a*, and DOM fluorescence continuous measurements from a scanning multiparametric probe (Idronaut, Italy) and a flow fluorometer designed at the P. P. Shirshov Institute of Oceanology, part of the Russian Academy of Sciences. The number of stations was increased in frontal zones with high horizontal gradients of surface salinity ( $S_0$ ). The sampling depths at the stations were defined after preliminary sounding of temperature, conductivity, and chlorophyll fluorescence using a CTD probe (SBE-19 and SBE-32, Seabird Electronics). Sampling was carried out using a carousel water sampler equipped with Niskin bottles. The data for Chl *a* and PP measured at discrete sampling depths are given in Online Resource 2.

## Measurement of PP

PP was estimated using a radiocarbon modification of the light and dark bottle method (Steemann Nielsen 1952). At three stations (5306, 5304\_2, and 5403), PP was determined in situ. Samples were taken in acid-cleaned 160-mL bottles and, after addition of sodium bicarbonate ( $\text{NaH}^{14}\text{CO}_3$ , 0.05  $\mu\text{Ci}$  per 1 mL of sample), were attached to a buoy and exposed outboard from solar culmination to sunset. After exposure, the samples were filtered onto 0.45- $\mu\text{m}$  nitrocellulose membrane (Vladipore, Russia). After filtration, samples were treated with 0.1 N HCl and filtered seawater, dried overnight, and placed in a scintillation vial with 10 mL scintillation cocktail (OptiPhase HiSafe III). The radioactivity

of the samples was determined after 24 h using a liquid scintillation counter (Triathler, Finland). Depth-integrated PP was calculated from the surface to the base of the photosynthetic zone using trapezoidal integration of the discrete depth values. The base of the photosynthetic zone is the horizon where PP measured in situ was equal to zero.

Samples at discrete depths were not taken at all stations. At other stations, indirect calculations of IPP were performed according to the modified method of Ryther and Yentsch (1957). Surface samples were exposed in a deck incubator with temperature maintained at in situ conditions. PP was calculated using the surface value ( $\text{PP}_0$ ), the vertical profile of Chl *a*, the underwater PAR, and the vertical distribution of the in situ chlorophyll-specific carbon fixation rate ( $P^b$ ) (Vedernikov et al. 1995). For PP calculations, we used the relationship between  $P^b$  and underwater PAR that was derived by averaging all in situ experiments performed in the Kara Sea from 1993 to 2016 (Fig. 2). For a specific site, measured vertical profiles of Chl *a* and underwater PAR were used. The vertical profile of  $P^b$  at that site was retrieved using the measured surface value and the average relative value taken from Fig. 2. The PP value at each sampling depth was calculated using measured Chl *a* and retrieved  $P^b$ . As seen in Fig. 2, the base of the photosynthetic zone in the Kara Sea coincides, in general, with the depth at which the underwater irradiance was equal to 0.25 % of surface PAR.

## Chl *a* determination

Chl *a* concentration was measured fluorometrically (Holm-Hansen et al. 1965). Seawater samples (500 mL) were

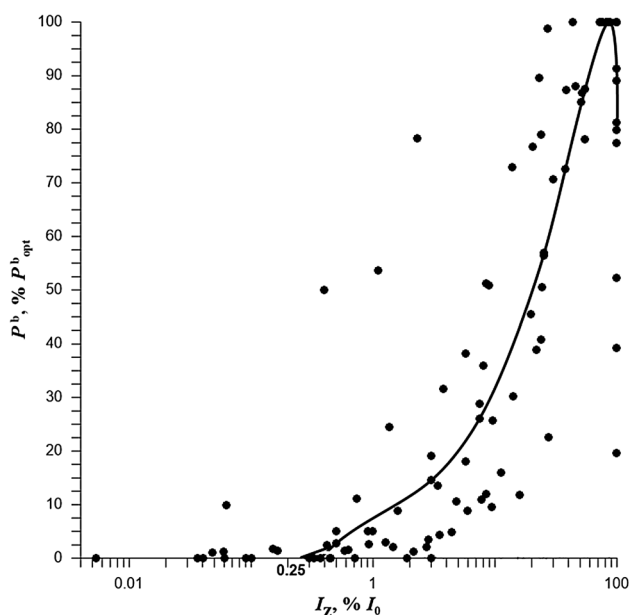


**Fig. 2** Relationship between chlorophyll-specific carbon fixation rate ( $P^b$ ) and photosynthetically available radiation at different depths ( $I_z$ ) obtained by averaging in situ experiments in the Kara Sea from 1993 to 2016

filtered onto Whatman GF/F glass fiber filters under low vacuum ( $\sim 0.3$  atm) and extracted in 90 % acetone (at  $5^\circ\text{C}$  in the dark for 24 h). The fluorescence of the extracts was measured using a fluorometer (Trilogy, Turner Designs) before and after acidification with 1 N HCl. The fluorometer was calibrated before and after the cruise using pure Chl *a* (Sigma) as standard. Concentrations of Chl *a* and pheophytin *a* (Pheo *a*) were calculated according to Holm-Hansen and Riemann (1978).

### Light measurements

The intensity of surface irradiance was measured using a LI-190SA (LI-COR) sensor mounted on the forecastle deck next to the sampling site. The daily PAR was obtained by integrating the results taken at 15-min intervals ( $\text{Ein m}^{-2}$ ) and were saved in the internal memory of the LI-1400 module. Underwater irradiance was measured at discrete depths (5 m in transparent water, 2 m in turbid water) within the euphotic zone using a LI-192SA (LI-COR) sensor. The diffuse attenuation coefficient for downwelling solar radiation in the visible spectrum ( $K_d$ ) was calculated according to Beer's law. In the absence of underwater hydrooptical measurements,  $K_d$  was calculated using empirical Kara Sea region-specific relationships between  $K_d$ , the Secchi depth ( $Z_S$ ), and  $\text{Chl}_0$  (Demidov et al. 2017a).

### Nutrient determination

Samples for determining pH, nutrients (silicates, phosphates, and nitrogen forms), and alkalinity were taken in 0.5-L plastic bottles without preservation, and were treated immediately after sampling. In areas with a considerable quantity of POM (estuaries and river–sea interfaces), the water samples were first filtered through a nuclear pore  $1\text{-}\mu\text{m}$  filter (Dubna, Russia). The contents of the main nutrients [ $\text{P-PO}_4$ ,  $\text{N-NO}_3$ ,  $\text{N-NO}_2$ ,  $\text{N-NH}_4$ , and  $\text{Si(OH)}_4$ ] were analyzed according to Grasshoff et al. (1999) and UNESCO (1983). Nitrates were reduced to nitrites using a column containing cadmium.  $\text{N-NO}_2$  concentration was measured using the Bendschneider and Robinson method.  $\text{N-NH}_4$  concentration was determined using a modified Solorzano method.  $\text{P-PO}_4$  concentration was measured using the Murphy and Riley method. Silicate was determined using the Strickland and Parsons method. Colorimetric determinations were performed using HACH Lange DR 2800 and LEKI SS2107UV spectrophotometers.

Total alkalinity (Alk) was determined using the direct titration method. Calculations of dissolved  $\text{CO}_2$  and various forms of dissolved inorganic carbon were performed by the pH-Alk method using thermodynamic equations for the carbon balance with constants for carbonic acid dissociation (Millero 1995; Hansen and Koroleff 1999) and corrections for low salinity (Makkaveev 1998).

### Determination of subsurface maxima and boundaries of mixed layer and nitracline

Following the approach of Brown et al. (2015), we define the SCM as a layer below the pycnocline where the CTD-mounted fluorometer registered increased values compared with overlying and underlying layers. SCM locations derived by discrete sampling were consistent with those obtained by sounding of fluorescence (Online Resource 3).  $\text{Chl}_{\text{max}}/\text{Chl}_0 \geq 1.15$ , where  $\text{Chl}_{\text{max}}$  is the depth with maximal Chl *a* concentration in the water column, was taken as an indicator of a well-pronounced SCM (Uitz et al. 2006). The SCM thickness was estimated according to the method of Martin et al. (2010).

The upper boundary of the subsurface PP maximum (SPM) was defined as the depth at which PP increased after decreasing in the upper layer. The depth of the maximal PP ( $\text{PP}_{\text{max}}$ ) was determined using the same approach as for  $\text{Chl}_{\text{max}}$ .

The horizon where the water density ( $\sigma_t$ ) exceeded the surface value by  $0.3 \text{ kg m}^{-3}$  was taken as the limit of the upper mixed layer (UML) (Timmermans et al. 2012). The distribution of nutrients in the UML was homogeneous. The upper boundary of the nitracline was determined from the depth of sharp increases in the sum of  $\text{N-NO}_2 + \text{N-NO}_3$ .

Below this boundary,  $N\text{-NO}_2 + N\text{-NO}_3$  concentrations exceeded the limiting value (Fisher et al. 1992; Tremblay et al. 2006).

## Results

### Spatial distribution of PP parameters

Along the Ob transect (Fig. 1), the  $\text{Chl}_0$  and the photosynthetic layer integrated Chl *a* concentration ( $\text{Chl}_{\text{ph}}$ ) varied by 3 and 2.5 orders of magnitude, from 0.05 to  $41.38 \text{ mg m}^{-3}$  and from 3.65 to  $148.52 \text{ mg m}^{-2}$ , respectively. In general, the values of  $\text{Chl}_0$  decreased from the Ob Estuary to the open sea (Fig. 3). The values of  $\text{Chl}_{\text{ph}}$  reached a maximum in the middle part of the estuary and gradually decreased northward to the open sea and southward to sites with null surface salinity (stations no. 5321\_2, 5323\_2, and 5324). The stations with pronounced SCM (stations no. 5307 and 5308) at the open part of the Ob transect were exceptions, where  $\text{Chl}_{\text{ph}}$  increased.

The spatial variability of IPP along the Ob transect was consistent with the spatial distribution of  $\text{Chl}_{\text{ph}}$ . The IPP values varied by a factor of 17, from 63 to  $1096 \text{ mgC m}^{-2} \text{ day}^{-1}$  (Fig. 3). The maximal chlorophyll-specific carbon

fixation rate ( $P_{\text{opt}}^b$ ) increased in the direction of the open sea (Fig. 4) and changed by a factor of 14, from 0.29 to  $4.12 \text{ mgC mg Chl } a^{-1} \text{ h}^{-1}$ . The exception was the distal point of the transect (station no. 5306), where  $P_{\text{opt}}^b$  declined by a factor of 3 compared with the adjacent station (station no. 5307). At station no. 5307, the lowest values of IPP and  $\text{Chl}_{\text{ph}}$  were observed, and a value of  $\text{Chl}_0$  close to the minimum was measured (Online Resource 1).

Along the Yenisey transect (Fig. 1),  $\text{Chl}_0$  increased from 0.07 to  $4.90 \text{ mg m}^{-3}$  (a factor of 70) while  $\text{Chl}_{\text{ph}}$  increased from 4.58 to  $36.22 \text{ mg m}^{-2}$  (a factor of 8). The values of these variables tended to decrease towards the open Kara Sea regions (Fig. 5). The twofold increase of  $\text{Chl}_{\text{ph}}$  at station no. 5350 can be explained by the SCM manifestation in the euphotic layer (Online Resource 3).

IPP along the Yenisey transect varied by one order of magnitude and was consistent with  $\text{Chl}_{\text{ph}}$  (Fig. 5). The values of IPP changed from 115 to  $1116 \text{ mgC m}^{-2} \text{ day}^{-1}$  (Online Resource 1). The values of  $P_{\text{opt}}^b$  along this transect varied by a factor of 2, from 1.29 to  $2.93 \text{ mgC mg Chl } a^{-1} \text{ h}^{-1}$ , and there was no trend that manifested in the distribution of this parameter (Fig. 6).

Along the transect of the western slope of the St. Anna Trough (Fig. 1), the variability of the PP characteristics was lower than along the Ob or Yenisey transects. The

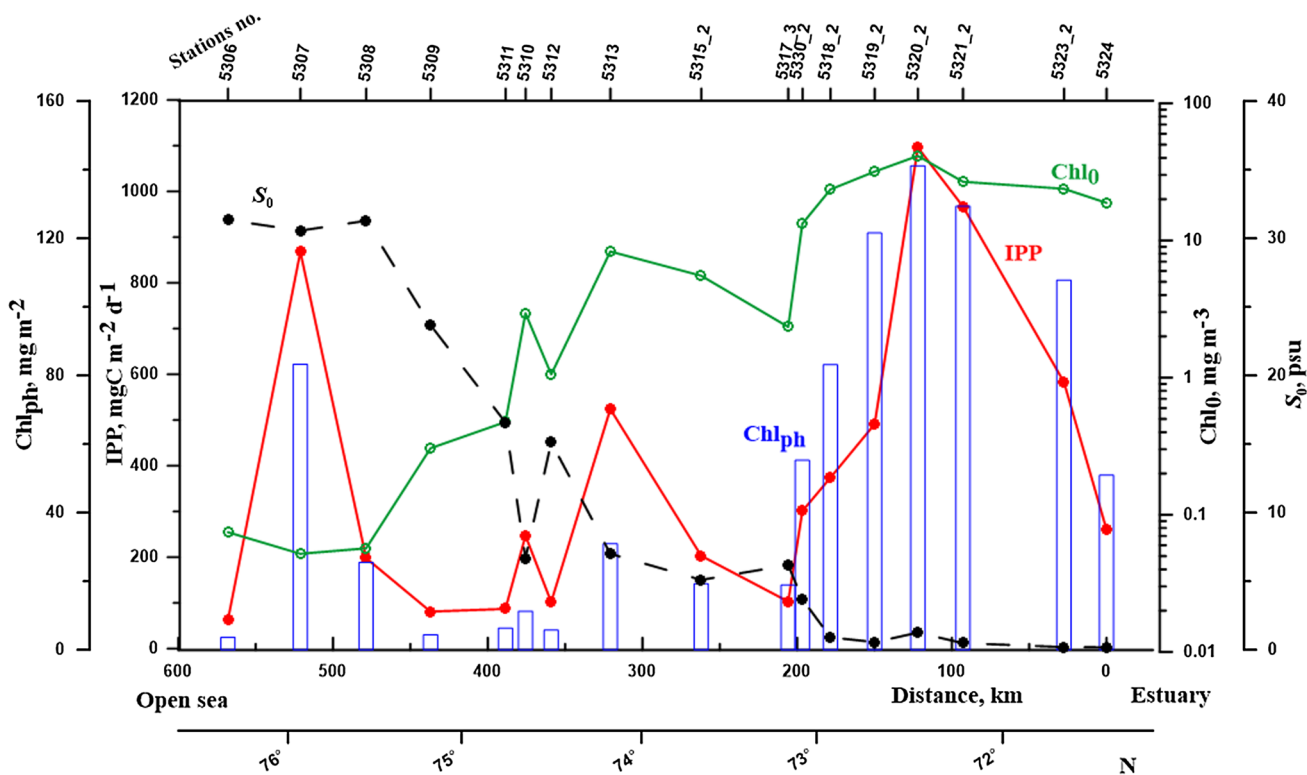


**Fig. 3** Spatial distribution of water column primary production (IPP), surface chlorophyll *a* concentration ( $\text{Chl}_0$ ), photosynthetic layer integrated chlorophyll *a* ( $\text{Chl}_{\text{ph}}$ ), and surface salinity ( $S_0$ ) along the Ob transect

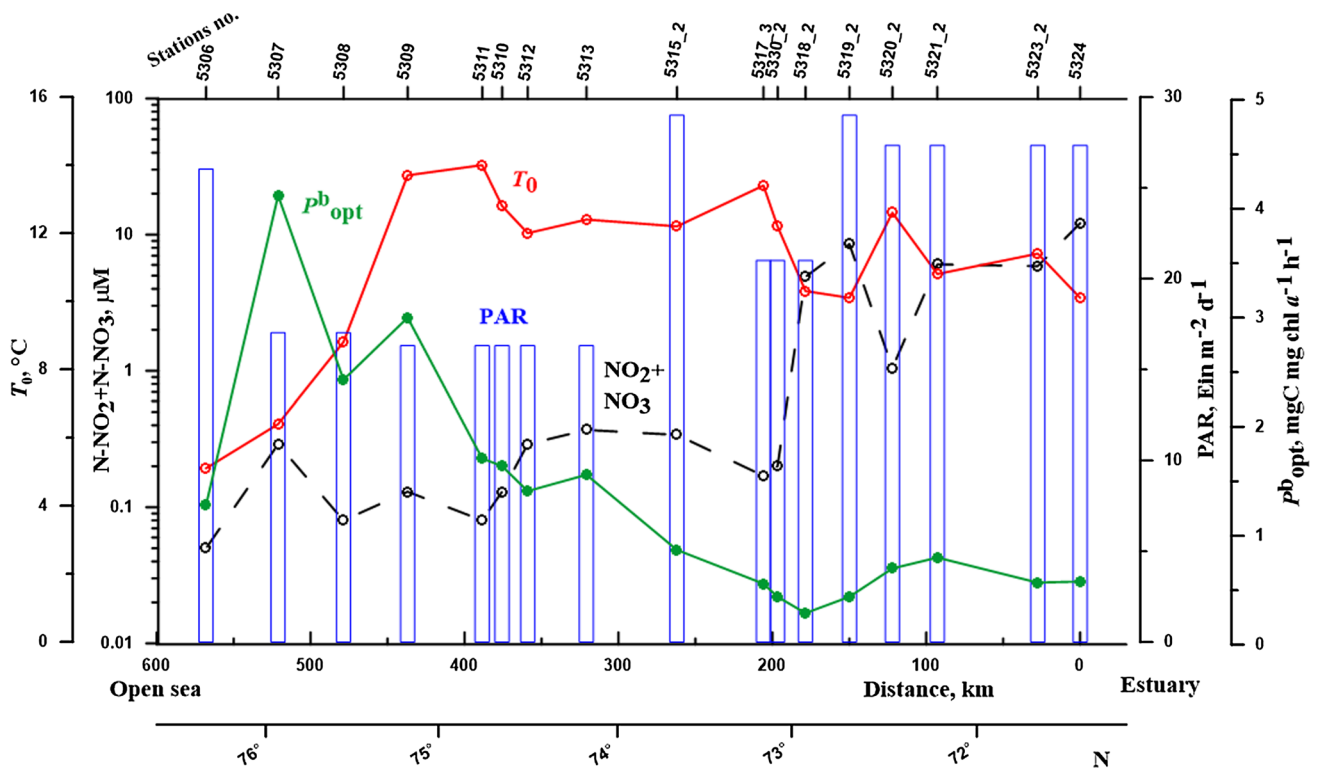


**Fig. 4** Spatial distribution of optimum chlorophyll-specific carbon fixation rate ( $P^b_{opt}$ ), surface water temperature ( $T_0$ ), sum of surface nitrite and nitrate ( $N\text{-NO}_2 + N\text{-NO}_3$ ), and photosynthetically available radiation (PAR) along the Ob transect

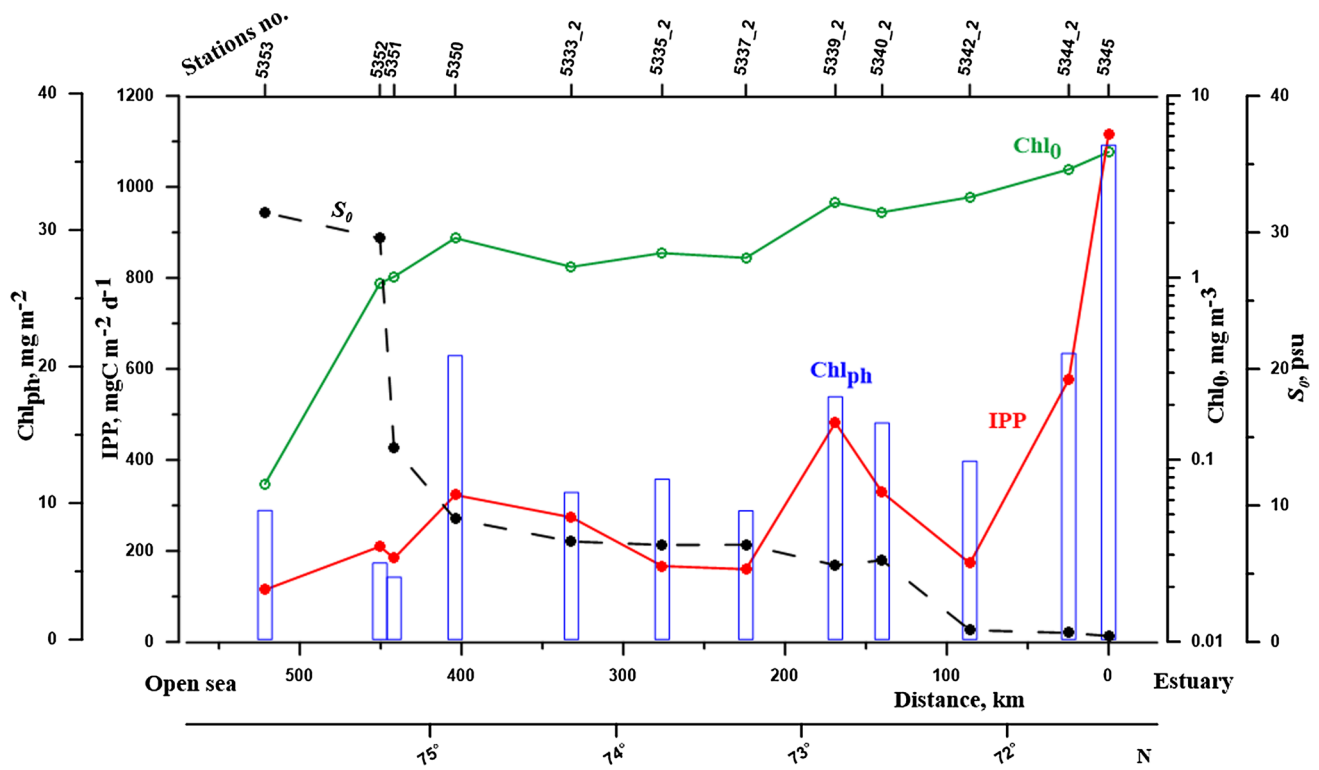


**Fig. 5** Spatial distribution of water column primary production (IPP), surface chlorophyll  $a$  concentration ( $Chl_0$ ), photosynthetic layer integrated chlorophyll  $a$  ( $Chl_{ph}$ ), and surface salinity ( $S_0$ ) along the Yenisey transect

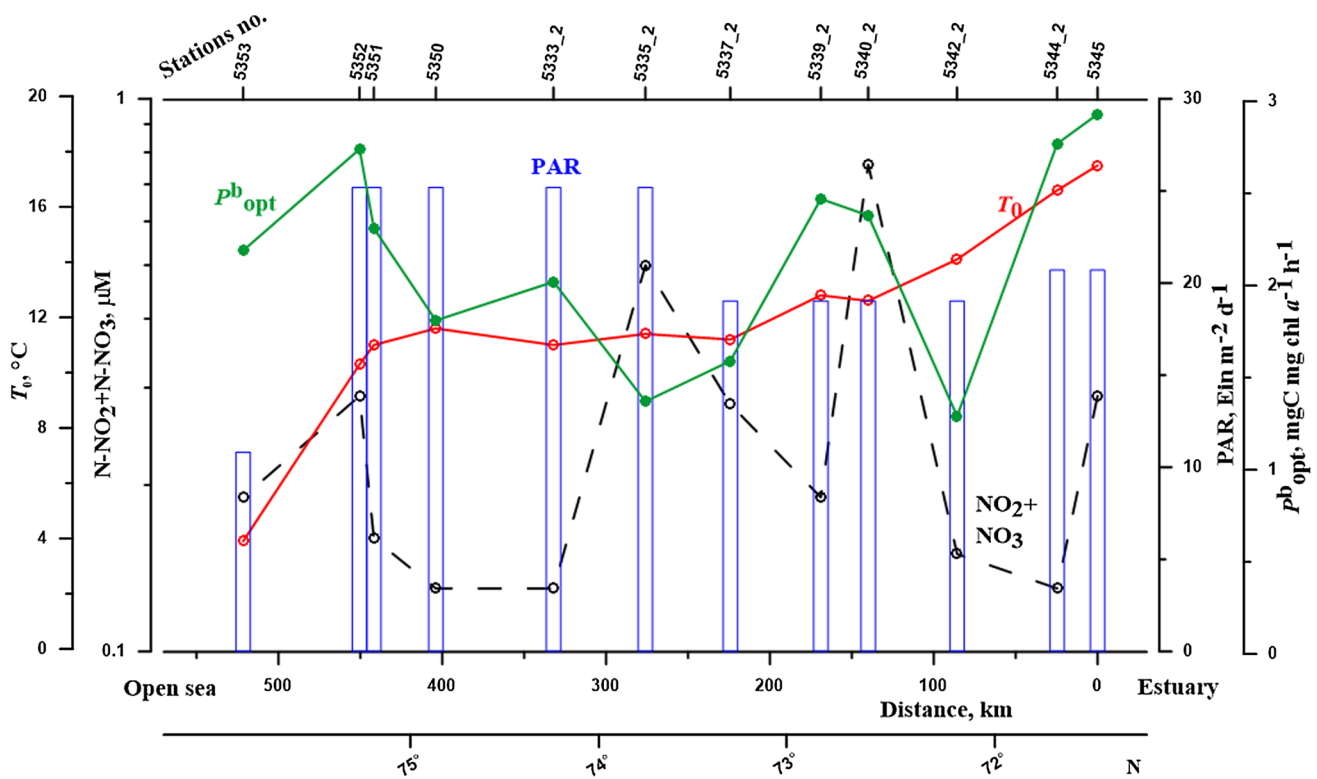


**Fig. 6** Spatial distribution of optimum chlorophyll-specific carbon fixation rate ( $P_{\text{opt}}^b$ ), surface water temperature ( $T_0$ ), sum of surface nitrite and nitrate ( $\text{N-NO}_2 + \text{N-NO}_3$ ), and photosynthetically available radiation (PAR) along the Yenisey transect

values of  $\text{Chl}_0$  and  $\text{Chl}_{\text{ph}}$  varied by factors of 5.5 and 3.5, from 0.10 to 0.54  $\text{mg m}^{-3}$  and from 8.70 to 30.14  $\text{mg m}^{-2}$ , respectively. IPP changed by a factor of 7, from 33 to 221  $\text{mgC m}^{-2} \text{day}^{-1}$ , and  $P_{\text{opt}}^b$  varied by a factor of 4, from 0.42 to 1.86  $\text{mgC mg Chl a}^{-1} \text{h}^{-1}$  (Online Resource 1).

In the western and southwestern parts of the Kara Sea (Fig. 1), the values of  $\text{Chl}_0$  and  $\text{Chl}_{\text{ph}}$  changed by factors of 53 and 7, from 0.03 to 1.60  $\text{mg m}^{-3}$  and from 4.46 to 32.19  $\text{mg m}^{-2}$ , respectively. The variability of IPP was close to one order of magnitude (from 54 to 514  $\text{mgC m}^{-2} \text{day}^{-1}$ ), while  $P_{\text{opt}}^b$  changed by a factor of 5 (from 1.32 to 6.50  $\text{mgC mg Chl a}^{-1} \text{h}^{-1}$ ) (Online Resource 1).

The variability of the productivity parameters can be related to their average values in salinity spans (Table 1). The average  $\text{Chl}_0$  values gradually decreased, and the depth of the photosynthetic layer ( $Z_{\text{ph}}$ ) increased; these changes were in accordance with the increase in surface salinity from the estuaries ( $S_0 = 0\text{--}5$  psu to  $S_0 > 25$  psu). In the ranges of 0–5, 6–10, and 11–25 psu, IPP and  $\text{Chl}_{\text{ph}}$  decreased as a result of the gradual decline of PP and  $\text{Chl a}$  from the estuaries towards the open sea (Figs. 3, 5). In waters with  $S_0 > 25$  psu, IPP and  $\text{Chl}_{\text{ph}}$  increased as a result of the SCM and SPM development and increase in  $Z_{\text{ph}}$  in the open waters (Table 1).

To explain the spatial distribution of PP and  $\text{Chl a}$ , it was necessary to determine the hydrometeorological conditions of the river plume development during the summer flood (June–September) and its propagation. The river plume dynamics were calculated using the particle-tracking model to trace the propagation of the river plume. This model uses satellite altimetry and reanalysis of wind data (Kubryakov et al. 2016). The model calculations (Fig. 7) suggested that, in June, July, and August, the river plume propagation had been of “central type” (Kubryakov et al. 2016) and its propagation to the west and north of the Kara Sea was minimal. The simulation results imply that, in the second half of August, the river plume propagation shifted to the east (Fig. 7). This type of river plume propagation was responsible for the location of the brackish waters close to the Ob and Yenisey Estuaries. These waters were characterized by high  $\text{Chl}_0$ ,  $\text{Chl}_{\text{ph}}$ , and IPP (Online Resource 1) values, and by a homogeneous vertical chlorophyll distribution. In contrast, waters in the west and southwest of the sea and unaffected by the rivers’ influence were characterized by low surface  $\text{Chl a}$  concentrations, and pronounced SCM with associated SPM. High values of IPP ( $>200$   $\text{mgC m}^{-2} \text{day}^{-1}$  and in some cases up to 500 and 800  $\text{mgC m}^{-2} \text{day}^{-1}$ ) in the western and southwestern regions can be explained mainly by the presence of SPM.

**Table 1** Statistics of phytoplankton primary production characteristics and abiotic factors in different salinity ranges

Range of $S_0$ , psu	Parameter							$N$
	IPP, $\text{mgC m}^{-2} \text{ day}^{-1}$	$\text{Chl}_0$ , $\text{mg m}^{-3}$	$\text{Chl}_{ph}$ , $\text{mg m}^{-2}$	$Z_{ph}$ , m	$\text{N-NO}_2 + \text{N-NO}_3$ , $\mu\text{M}$	$\text{P-PO}_4$ , $\mu\text{M}$	$\text{Si(OH)}_4$ , $\mu\text{M}$	
0–5	$649 \pm 326$ (173–1116)	$22.35 \pm 12.82$ (2.76–41.38)	$86.05 \pm 47.49$ (13.06–148.52)	$5 \pm 1$ (3–7)	$3.61 \pm 3.83$ (0.13–12.14)	$0.50 \pm 0.42$ (0.05–1.44)	$133.9 \pm 49.2$ (64.1–213.0)	13
6–10	$281 \pm 137$ (103–524)	$2.94 \pm 2.27$ (1.15–8.30)	$16.67 \pm 6.45$ (9.44–30.92)	$8 \pm 2$ (5–11)	$0.30 \pm 0.20$ (0.13–0.76)	$0.07 \pm 0.08$ (0–0.25)	$87.49 \pm 37.36$ (52.15–143.99)	10
11–25	$114 \pm 48$ (81–184)	$0.71 \pm 0.38$ (0.31–1.05)	$5.25 \pm 0.93$ (4.37–6.31)	$14 \pm 2$ (11–17)	$0.17 \pm 0.09$ (0.08–0.29)	$0.06 \pm 0.05$ (0.02–0.13)	$64.09 \pm 21.29$ (33.21–78.61)	4
>>25	$176 \pm 183$ (33–868)	$0.22 \pm 0.36$ (0.03–1.60)	$17.35 \pm 16.32$ (3.65–83.28)	$43 \pm 13$ (17–67)	$0.25 \pm 0.21$ (0.05–0.80)	$0.08 \pm 0.04$ (0.02–0.14)	$2.47 \pm 5.96$ (0.21–29.84)	24

Data presented as mean  $\pm$  standard deviation (limits)

IPP water column primary production,  $\text{Chl}_0$  surface Chl *a* concentration,  $\text{Chl}_{ph}$  photosynthetic layer integrated Chl *a* concentration,  $Z_{ph}$  photosynthetic depth,  $\text{N-NO}_2 + \text{N-NO}_3$ ,  $\text{P-PO}_4$ ,  $\text{Si(OH)}_4$  surface concentrations of the sum of nitrite and nitrate, phosphate, and dissolved silica, respectively,  $S_0$  surface salinity,  $N$  number of data

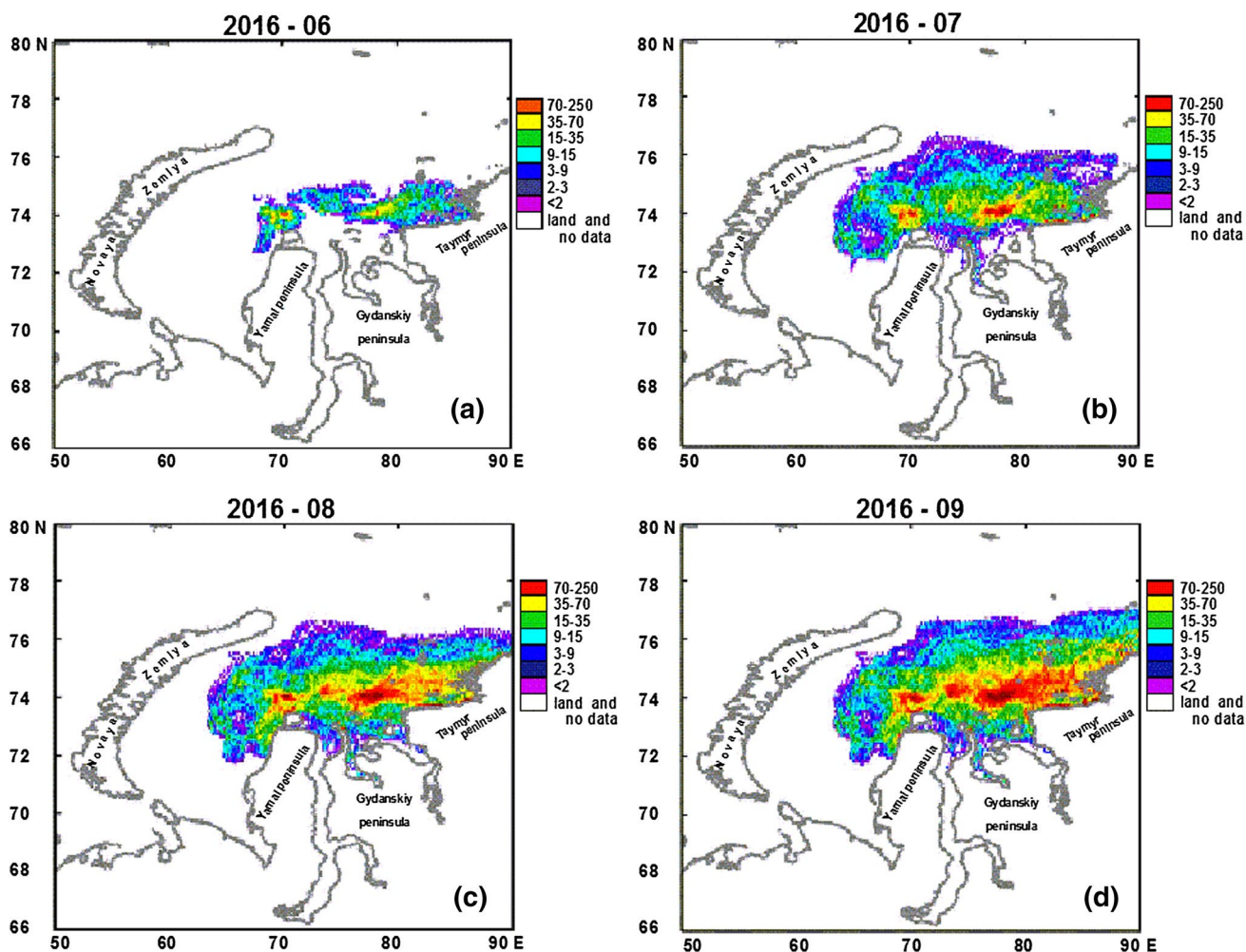


**Fig. 7** Distribution of virtual particle concentration calculated by particle-tracking model for pathways of plume propagation (Kubryakov et al. 2016) in June (a), July (b), August (c), and September (d) 2016

## Vertical variability of chlorophyll and PP

The existence of SCM and SPM was a characteristic of the vertical distribution of chlorophyll and PP in the Kara Sea from July to August. In general, SCM were observed at 24 sites (47 % of the total number of stations). SCM were registered at all stations in the western and southwestern areas of the Kara Sea, with the exception of station no. 5404 in the vicinity of Vaygach Island (12 sites, 50 % of the stations with SCM). The rest of the sites with SCM were located in the offshore parts of the Ob and Yenisey transects. The main characteristics of SCM and SPM are presented in Table 2. There were no SCM in the Ob and Yenisey Estuaries or in the St. Anna Trough, with the exception of station no. 5306\_2 (Fig. 1).

Thus, all the stations can be divided into two types: with SCM (type A) (Fig. 8) and without SCM (type B) (Fig. 9). The positions of SPM varied in relation to SCM. At type A stations, the main PP peak was located near the surface, and a less pronounced ancillary peak was associated with SCM (Fig. 8a, b). At some stations, a single near-surface PP maximum was registered, and there were no SPM at the depths of SCM (Fig. 8c). In other cases, there was a pronounced association between the main SPM and SCM (Fig. 8d–f) at the base of the euphotic zone (1 % PAR). Type A stations were located in the west and southwest of the Kara Sea and at the northern part of the Ob transect. At these (type A) stations, SCM were developed at low surface Chl *a* concentrations ( $\text{Chl}_0 \leq 0.10 \text{ mg m}^{-3}$ ) (Online Resource 1).

Type B stations were characterized by either near-bottom increasing Chl *a* without SPM (Fig. 9a, b) or gradually decreasing Chl *a* concentrations with depth (Fig. 9c–f). At type B stations, a maximum PP was observed near the surface. Type B stations characterized by near-bottom  $\text{Chl}_{\text{max}}$  were located on the shelf in the middle of the Ob transect. There were no SPM associated with near-bottom Chl *a* increasing at those sites (Fig. 9a, b). The stations where Chl *a* concentrations gradually decreased with depth (Fig. 9c–f) were mainly located on the Ob–Yenisey shoal or in the St. Anna Trough.

## Discussion

### Influence of main environmental factors on PP during July–August 2016

Nutrient concentrations, and incident and underwater PAR are the main abiotic factors that limit PP in the Arctic Ocean (Sakshaug 2004). It has also been shown that, in the oligotrophic open Kara Sea in autumn, incident PAR, nutrients, temperature, and high water turbidity constrain the PP of phytoplankton (Vedernikov et al. 1995).

Based on literature sources, we took the following values of  $\text{N-NO}_2 + \text{N-NO}_3$ ,  $\text{P-PO}_4$ , and  $\text{Si(OH)}_4$  as the limiting concentrations: 0.9, 0.5, and 2  $\mu\text{M}$ , respectively (Egge and Aksnes 1992; Fisher et al. 1992; Tremblay et al. 2006). As shown in Table 3 and Online Resource 1, during the study period, the  $\text{N-NO}_2 + \text{N-NO}_3$  and  $\text{P-PO}_4$  concentrations exceeded the limiting values only in the Ob and Yenisey Estuaries. In contrast, the concentrations of dissolved silica were, on average, higher than the limiting values. Thus, in the second half of July and in the beginning of August, dissolved nitrogen and phosphorus could constrain phytoplankton growth.

Light conditions are considered to be one of the main factors limiting PP in the Arctic Ocean in spring and summer (Hill and Cota 2005; Lee and Whitledge 2005; Ardyna et al. 2011). It has been shown that insolation is the main factor controlling the PP rate in the Kara Sea at the end of the growing season (Demidov et al. 2014). During the study period, the level of underwater PAR ( $I_0$ ) was high, ranging from 9 to 39  $\text{Ein m}^{-2} \text{ day}^{-1}$ . This finding, as well as the lack of correlation between IPP and  $I_0$ , and between  $P_{\text{opt}}^{\text{b}}$  and  $I_0$  ( $R^2 = 0.01$  and 0.04, respectively) indicates that, in the middle of summer, PAR was not a limiting factor for PP in the Kara Sea.

Currently, Arctic Ocean IPP estimations are often conducted on the basis of the Chl *a* concentration as a single parameter (Hill and Zimmerman 2010; Hill et al. 2013; Matri et al. 2013). When applying this estimation, it is important to determine the relationship between IPP and Chl *a*. In previous work, it was shown that, in autumn, IPP primarily depends on the assimilation activity rather than the chlorophyll-specific biomass (Demidov et al. 2014). In the middle of summer, the opposite results were obtained. Correlation analysis showed that, in July–August, IPP was closely linked with surface and depth-integrated Chl *a* ( $R^2 = 0.50$  and 0.61,  $p < 0.05$ , respectively). Consequently, there was no reliable relationship between IPP and  $P_{\text{opt}}^{\text{b}}$  ( $R^2 = 0.04$ ).

### Influence of vertical chlorophyll distribution on water column primary production

In July and August 2016, IPP mainly depended on the vertical Chl *a* distribution. We reached this conclusion based on the high contributions of SCM to IPP. According to a study using autumn data, the SCM integrated PP contributed, on average, from 1 to 27 % to IPP (Demidov et al. 2014), and from 60 to 88 % of IPP was produced within the UML (Demidov and Mosharov 2015). A highly unusual situation was observed in the summer of 2016, when  $\text{Chl}_{\text{max}}$  exceeded  $\text{Chl}_0$  by up to two orders of magnitude (station no. 5307) and SPM contributed >30 % to water column IPP (Table 2).

Around the Arctic Ocean, SCM are common features in summer and autumn (Cota et al. 1996; Hill and Cota 2005;

**Table 2** Characteristics of subsurface chlorophyll maximum (SCM) and subsurface primary production maximum (SPM) in the Kara Sea in July–August 2016

Station no.	Chl <sub>max</sub> , mg m <sup>-3</sup>	Depth of Chl <sub>max</sub> , m	Chl <sub>max</sub> /Chl <sub>0</sub>	Vertical scale of SCM, μm	Limits of SCM, m	PP <sub>max</sub> , mgC m <sup>-3</sup> day <sup>-1</sup>	Depth of PP <sub>max</sub> , m	PP <sub>max</sub> /PP <sub>0</sub>	IPP <sub>SCM</sub> /IPP, %	Pheo <i>a</i> , %
5302	1.27	35	38.11	40	20–60	25.73	35.0	6.2	83	22
5303	0.85	42	23.84	30	25–55	3.43	35.0	3.8	69	23
5305	2.23	40	88.01	50	20–70	17.13	33.0	7.6	84	16
5306	0.30	12	4.08	16	2–18	5.38	8.0	2.4	95	26
5307	10.11	35	194.64	15	25–40	94.86	35.0	23.1	86	9
5308	1.98	35	34.82	15	25–40	13.31	35.0	5.0	73	18
5306_2	1.01	42	9.88	45	15–60	7.64	30.0	2.1	81	21
5358	0.84	40	28.59	20	30–50	4.76	40.0	2.0	37	16
5299	0.40	18	1.64	30	10–40	28.02	1.5	1.3	31	32
5304_2	0.84	45	10.18	23	35–58	3.46	5.0	3.4	12	16
5304	5.15	50	154.20	25	35–60	2.94	15.0	1.5	13	14
5353	0.68	60	9.30	15	40–55	4.80	20.0	1.6	0 <sup>a</sup>	32
5357	1.21	54	17.22	43	22–65	4.54	1.2	1.9	34	38
5392	0.39	45	6.79	30	30–60	3.14	1.0	1.3	4	35
5394	0.40	28	3.75	23	20–43	11.14	1.2	1.2	35	32
5403	0.72	25	4.02	32	8–40	5.77	1.5	1.3	61	22
5299_2	0.52	30	1.80	62	8–70	7.21	1.0	1.1	49	32
5309	7.09	30	23.17	13	17–30	20.39	0.5	1.2	0 <sup>a</sup>	7
5310	4.69	27	1.59	12	15–27	115.85	0.2	1.3	0 <sup>a</sup>	10
5311	1.74	27	3.66	9	18–27	19.52	0.4	1.3	0 <sup>a</sup>	24
5312	1.71	27	1.62	17	10–27	35.63	0.3	1.3	0 <sup>a</sup>	23

Chl<sub>max</sub> maximal Chl *a* concentration within SCM, Chl<sub>max</sub>/Chl<sub>0</sub> ratio of maximal Chl *a* concentration within SCM to surface Chl *a* concentration, PP<sub>max</sub> maximal value of primary production in water column, PP<sub>max</sub>/PP<sub>0</sub> ratio of maximal value of primary production to surface value of primary production, IPP<sub>SCM</sub>/IPP ratio of SCM integrated primary production to water column primary production, Pheo *a* pheophytin *a* content in relation to sum of Chl *a* and Pheo *a* at depth of Chl<sub>max</sub>

<sup>a</sup>The null of the IPP<sub>SCM</sub>/IPP ratio was observed at stations where SCM was located below the photosynthetic layer

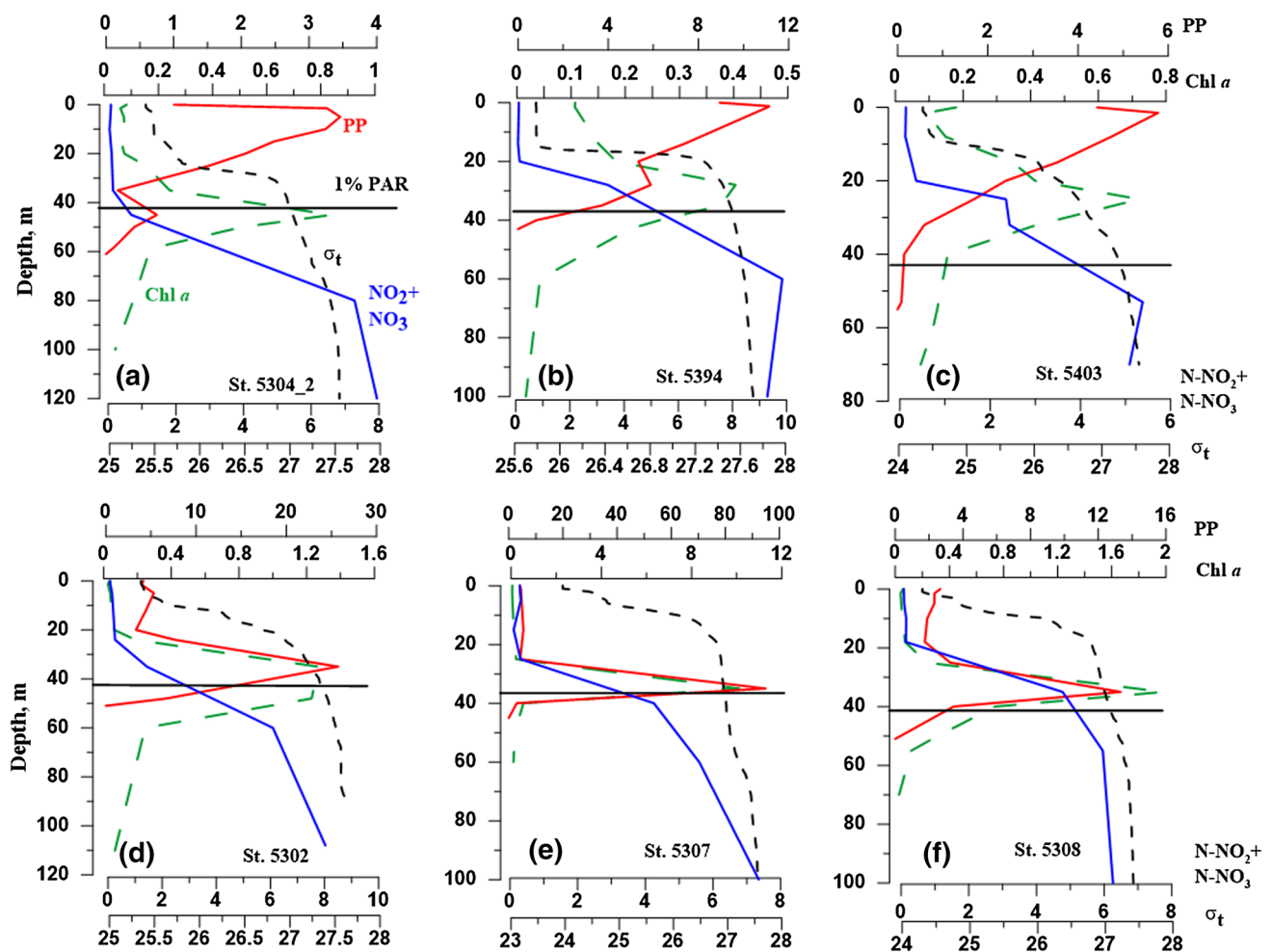


**Fig. 8** Vertical distribution of primary production (PP,  $\text{mgC m}^{-3} \text{ day}^{-1}$ ), chlorophyll *a* concentration (Chl *a*,  $\text{mg m}^{-3}$ ), sum of nitrite and nitrate ( $\text{N-NO}_2 + \text{N-NO}_3$ ,  $\mu\text{M}$ ), and water density ( $\sigma_t$ ,  $\text{kg m}^{-3}$ ) at stations with well-pronounced subsurface chlorophyll

maximum (SCM). **a–c** stations with PP maximum within the surface layer; **d–f** stations where the subsurface PP maximum (SPM) was associated with SCM. The horizontal line denotes the boundary of the euphotic layer (1 % of PAR)

Martin et al. 2010; 2012; Arrigo et al. 2011; Ardyna et al. 2013; Cherkasheva et al. 2013; Brown et al. 2015). SCM is formed by the sinking of the vernal bloom or as a result of the photoadaptive reaction of phytoplankton to low light intensity. The Arctic Ocean follows global patterns (Cullen 2015) and SCM develop within the nutricline at the boundary of the euphotic zone (1 % of  $I_0$ ). The phytoplankton growth at these depths results from a compromise between the nutrient supply and the level of underwater irradiance, which is close to the compensation point. In contrast with general global and Arctic Ocean patterns, the results from Kara Sea autumn expeditions have shown that, in the Kara Sea, SCM was weakly pronounced and the Chl *a* maximum was located at the surface (Demidov et al. 2014; Demidov and Mosharov 2015). Measurements that formed the basis of the earlier generalizations were carried out in 1993, 2007, and 2011. In those years, a river plume was

observed over an extensive area of the Kara Sea and the so-called western-type plume propagation was identified (Kubryakov et al. 2016). As a result, the brackish waters of the river plume were observed in the western and southwestern parts of the Kara Sea. In these waters, high DOM and POM concentrations, as well as high surface Chl *a* ( $> 1.0 \text{ mg m}^{-3}$ ) were the causes of the low water transparency and shallow depth of the euphotic layer (Hanzlick and Aagaard 1980; Stein 2000; Dittmar and Kattner 2003; Amon 2004; Rachold et al. 2004; Vetrov and Romankevich 2004; Holmes et al. 2012; Le Fouest et al. 2013). These conditions were not favorable for SCM development in 1993, 2007, and 2011. However, in the summer of 2016, the river plume, as mentioned above, was observed to be opposite to the Ob and Yenisey Estuaries (Fig. 7), and did not restrict SCM development in the western and southwestern parts of the Kara Sea under conditions of low

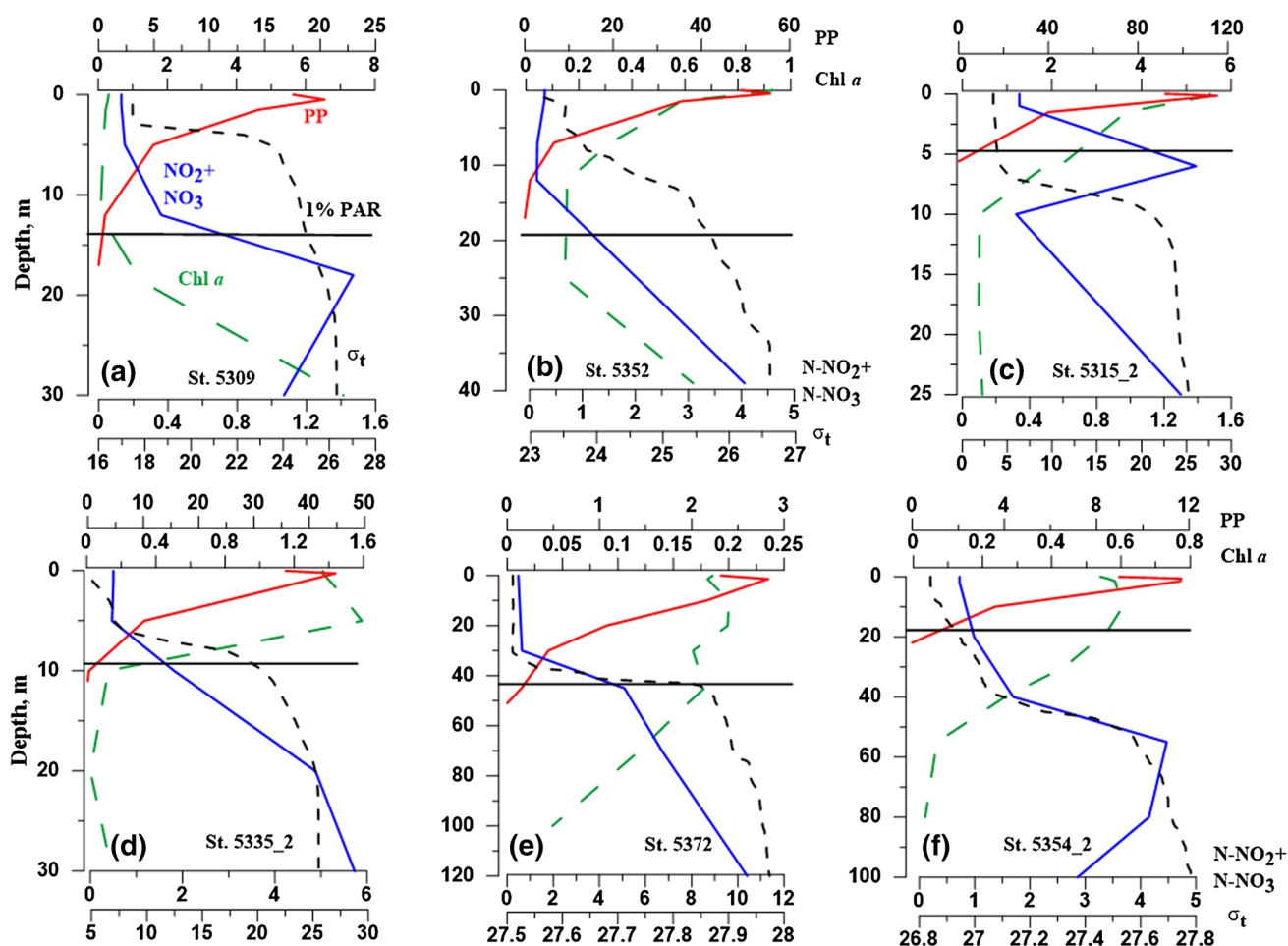


**Fig. 9** Vertical distribution of primary production (PP,  $\text{mgC m}^{-3} \text{ day}^{-1}$ ), chlorophyll *a* concentration (Chl *a*,  $\text{mg m}^{-3}$ ), sum of nitrite and nitrate ( $\text{N-NO}_2 + \text{N-NO}_3$ ,  $\mu\text{M}$ ), and water density ( $\sigma_t$ ,  $\text{kg m}^{-3}$ ) at stations without well-pronounced subsurface chlorophyll

maximum (SCM). **a–d** stations in the river runoff region; **e, f** stations on the western slope of the St. Anna Trough. The horizontal line denotes the boundary of the euphotic layer (1 % of PAR)

surface Chl *a* ( $\leq 0.1 \text{ mg m}^{-3}$ ) and high water transparency ( $Z_S > 15 \text{ m}$ ).

Environmental conditions strongly determine SCM and SPM development. The values of the abiotic parameters that were determined at the depths of SCM and SPM are presented in Table 3. The values of Chl<sub>max</sub> were mainly measured at depths below the UML and the upper boundary of the nitracline. The  $\text{N-NO}_2 + \text{N-NO}_3$  concentrations at the depth of Chl<sub>max</sub> were higher than the limiting value in 67 % of cases. Limiting concentrations of  $\text{N-NO}_2 + \text{N-NO}_3$  at that depth were measured when the chlorophyll maximum was registered within the UML. This occurred near the seabed or at sites where the upper boundary of the nitracline was close to Chl<sub>max</sub> (Table 3). Thus, high  $\text{N-NO}_2 + \text{N-NO}_3$  values within the SCM suggest that there was no nutrient limitation in this layer. Low Pheo *a* concentrations at these depths ( $\leq 38 \%$ ) (Table 2) imply that the phytoplankton communities were in perfectly functional condition.

When the light conditions at the SCM are considered, it is noted that the depth of Chl<sub>max</sub> was located close to the boundary of the euphotic layer (1 % of PAR) and the compensation depth ( $Z_{\text{ph}}$ ). The absolute PAR values at most sites were lower than  $1 \text{ Ein m}^{-2} \text{ day}^{-1}$ . In three cases, when the Chl<sub>max</sub> concentrations were determined to be within well-lit layers close to the UML (stations no. 5306, 5335\_2, and 5333\_2), the PAR values ranged from 1.14 to  $5.15 \text{ Ein m}^{-2} \text{ day}^{-1}$ . At shoal sites, the SCM were located near the bottom at zero PAR (Table 3).

These findings allow us to propose two hypotheses that need to be tested in further studies. First, the light and nutrient conditions for SCM development in the Kara Sea were the same as in other regions of the Arctic Ocean (Martin et al. 2010; 2012; Brown et al. 2015). Second, phytoplankton communities within SCM were viable. SCM in the middle of summer (July and first half of August) in the Kara Sea were not formed by the sinking

**Table 3** Environmental characteristics of subsurface chlorophyll maximum in the Kara Sea in July–August 2016

Station no.	Depth of Chl <sub>max</sub> , m	UML, m	Z <sub>pd</sub> , m	Z <sub>nit</sub> , m	N-NO <sub>2</sub> + N-NO <sub>3</sub> at depth of Chl <sub>max</sub> , μM	Absolute I <sub>z</sub> at depth of Chl <sub>max</sub> , Ein m <sup>-2</sup> day <sup>-1</sup>	Relative I <sub>z</sub> at depth of Chl <sub>max</sub> , %	Absolute I <sub>z</sub> at depth of PP <sub>max</sub> , Ein m <sup>-2</sup> day <sup>-1</sup>	Relative I <sub>z</sub> at depth of PP <sub>max</sub> , %
5302	35	10	9	24	1.44	0.27	2.30	0.27	2.30
5303	42	10	9	25	5.03	0.40	1.12	0.84	2.36
5305	40	9	8	20	6.01	0.16	0.60	0.38	1.46
5306	12	7	7	4	3.43	5.15	19.79	5.15	19.79
5307	35	6	8	25	3.27	0.22	1.30	0.22	1.30
5308	35	5	9	18	4.77	0.33	1.94	0.33	1.94
5306_2	42	20	10	22	4.41	0.16	1.50	0.57	5.24
5358	40	20	8	30	2.83	0.29	0.74	0.29	0.74
5299	18	5	5	28	0.17	0.33	2.83	8.60	74.30
5304_2	45	14	8	40	0.68	0.17	0.63	13.83	52.73
5304	50	9	8	35	4.71	0.06	0.17	6.17	17.30
5353	60	14	7	17	4.94	0.01	0.12	0.74	6.86
5357	54	24	8	40	4.16	0.04	0.10	33.60	85.74
5392	45	14	6	30	7.5	0.82	4.33	16.19	85.74
5394	28	15	8	20	3.4	0.27	2.78	8.30	85.74
5403	25	8	7	20	2.35	0.59	2.83	16.80	80.57
5299_2	30	9	6	12	1.01	0.10	0.63	13.62	85.74
5309	30	3	3	9	1.07	0.00	0.01	13.98	85.74
5310 <sup>a</sup>	27	2	1	–	0.34	0.00	0.00	13.98	85.74
5311 <sup>a</sup>	27	3	2	–	0.18	0.00	0.00	13.98	85.74
5312 <sup>a</sup>	27	3	2	–	0.15	0.00	0.00	13.98	85.74

UML upper mixed layer, Z<sub>pd</sub> penetration depth ( $Z_{pd} = 1/K_d$ , where  $K_d$  is the diffuse attenuation coefficient for downwelling radiation), Z<sub>nit</sub> depth of the upper boundary of the nitracline, N-NO<sub>2</sub> + N-NO<sub>3</sub> at depth of Chl<sub>max</sub> concentration of the sum of nitrite and nitrate, I<sub>z</sub> photosynthetically available radiation at depth Z

<sup>a</sup>There was no manifested nitracline at stations no. 5310–5312

of the phytoplankton bloom from the surface as a result of nutrient exhaustion.

As mentioned above, SCM and SPM located at different depths and the environmental conditions for SPM development inside and outside the layer of Chl<sub>max</sub> could be different. As shown in Table 3, PAR was low (0.22–0.84 Ein m<sup>-2</sup> day<sup>-1</sup>) at the stations where the main maximum of the PP that exceeded PP<sub>0</sub> was located close to the depth of Chl<sub>max</sub> (30–40 m). The exception was station no. 5306 because of the shallow boundary of the nitracline and the high position of Chl<sub>max</sub> in the water column. These low PAR values were lower than the compensation intensity of light for Arctic Ocean phytoplankton (1.3–1.9 Ein m<sup>-2</sup> day<sup>-1</sup>) (Tremblay et al. 2006; Tremblay and Gagnon 2009). The assimilation activity in SPM was also low (0.18–0.85 mgC mg Chl a<sup>-1</sup> h<sup>-1</sup>). The high level of PP under such conditions was provided by the high chlorophyll-specific phytoplankton biomass.

At other stations, SPM were mainly observed within well-lit subsurface layers (8.6–21.6 Ein m<sup>-2</sup> day<sup>-1</sup>). As can be observed in Table 3, the significant (> 60 %) contribution of SPM-integrated PP to the water column IPP occurs in two

cases. First, when the chlorophyll-specific biomass within the SPM is formed under conditions of low irradiance and assimilation activity but with favorable nutrition. Second, a productive layer has a high Chl *a* content, but less than Chl<sub>max</sub>, and it is close to the surface within the well-lit zone.

IPP estimations with satellite-derived data are carried out using the average Chl *a* within the penetration depth ( $Z_{pd} = 1/K_d$ , where  $K_d$  is the diffuse attenuation coefficient for downwelling PAR). As shown in Tables 2 and 3,  $Z_{pd} \ll Z$  of Chl<sub>max</sub> and Z of PP<sub>max</sub> when the latter is associated with SCM. Therefore, in our case, a significant part of IPP created below Z<sub>pd</sub> can be missed in the model calculations with satellite-derived Chl *a* as an input variable. Our findings are supported by earlier work that identified divergences between model and field IPP observations at sites with well-pronounced SCM and SPM (Arrigo et al. 2011; Ardyna et al. 2013; Hill et al. 2013). However, there are different opinions regarding the role of SCM in Arctic Ocean IPP estimations. Some authors emphasize that postbloom SCM facilitate SPM development or smooth the vertical profiles of PP, thus significantly affecting annual IPP (Zhai et al. 2012; Hill et al. 2013). Other authors have shown that the SPM contribution

to annual IPP is negligible (Arrigo et al. 2011; Ardyna et al. 2013). The results of previous Kara Sea studies carried out in autumn suggested that SPM associated with SCM affects IPP in specific cases (Demidov and Mosharov 2015). However, when the average vertical Chl *a* distribution is taken into account, the contribution of subsurface maxima to the IPP is insignificant (Demidov et al. 2017a). Data presented here reveal that, in the middle of summer in the Kara Sea, SCM and SPM contributed a significant part to water column PP at certain stations. It would appear that, in summer, the influence of SPM on IPP is considerably higher than in autumn. Nevertheless, we cannot currently estimate the role of SCM for the total Kara Sea IPP in summer because of undersampling. Detailed studies of the nature of the Kara Sea SCM are needed. These studies should be focused on the structure and functional conditions of phytoplankton communities in SCM.

## Conclusions

For the first time, the spatial variability of primary production characteristics in the middle of summer was studied over the vast Kara Sea area. Our results allow comparison of the features of Kara Sea primary production in summer and in autumn:

1. At the end of July and beginning of August, for the first time, extremely low values of Chl<sub>0</sub> (<0.1 mg m<sup>-3</sup>) were derived in the west and southwest of the Kara Sea, in contrast to autumn when the surface Chl *a* concentration was always more than 0.1 mg m<sup>-3</sup>.
2. In summer, a close relationship between IPP and Chl *a* content was established, as evidenced by high determination coefficients between Chl<sub>0</sub> and IPP, and between Chl<sub>ph</sub> and IPP ( $R^2 = 0.50$  and  $0.61$ , respectively). In contrast, in autumn, primary production in the Kara Sea mainly depended on the physiological state of phytoplankton, particularly on the assimilation activity rather than chlorophyll-specific biomass.
3. In the middle of summer under good light conditions, due to the relatively high solar angle and polar day, incident PAR was not a limiting factor. As shown in previous work (Demidov et al. 2014), at the end of the growing season, primary production depended mainly on PAR.
4. At the end of July and beginning of August in the open Kara Sea, well-pronounced SCM were observed. SCM often accompanied primary production maxima. In that case, SPM contributed more than 30 % to water column primary production. In contrast, the vertical distributions of PP and Chl *a* in the Kara Sea in autumn

were characterized by surface maxima and gradually decreased with depth.

Thus, in July–August, the patterns of primary production in the Kara Sea were different from those studied in autumn (Bobrov et al. 1989; Vedernikov et al. 1995; Mosharov 2010; Demidov et al. 2014; Mosharov et al. 2016). Further investigations of primary production in the Kara Sea at the beginning of the growing season are needed to improve knowledge about its seasonal cycle and the correction of annual IPP estimations.

**Acknowledgements** We thank Paul Seward, PhD, from Edanz Group ([www.edanzediting.com/ac](http://www.edanzediting.com/ac)) for editing a draft of this manuscript. We thank the crew of the R/V “Akademik Mstislav Keldysh” for their cooperation during the 66th cruise. We are grateful to the GSFC (Goddard Space Flight Center, Distributed Active Archive Center) at NASA for the MODIS-Aqua data and The Arctic Great Rivers Observatory (Arctic-GRO) project for Ob and Yenisey discharge data. Thanks are given to A. A. Kubryakov and S. S. Stanichny for calculations of river plume dynamics. This work was supported by the Russian Foundation for Fundamental Research (project no. 16-05-00050). Expeditionary observations and sample treatments were supported by the Russian Science Foundation (project no. 14-50-00095, scientific direction “Ecosystems of strategically important marine regions of Russian Federation”). The application of optic data were supported by the Russian Science Foundation (project no. 14-50-00095, scientific direction “Interaction of physical, biological and geological processes at coastal zone, shore waters and inland seas”).

## References

- Amon RMW (2004) The role of dissolved organic matter for the organic carbon cycle in the Arctic Ocean. In: Stein R, Macdonald RW (eds) The organic carbon cycle in the Arctic Ocean. Springer, Berlin, pp 83–100
- Anonymous (1958) The Venice System for the classification of marine waters according to salinity. *Limnol Oceanogr* 3:346–347
- Ardyna M, Gosselin M, Michel C, Poulin M, Tremblay JÉ (2011) Environmental forcing of phytoplankton community structure and function in the Canadian High Arctic: contrasting oligotrophic and eutrophic regions. *Mar Ecol Progr Ser* 442:37–57
- Ardyna M, Babin M, Gosselin M, Devred E, Bélanger S, Matsuoka A, Tremblay JÉ (2013) Parameterization of vertical chlorophyll *a* in the Arctic Ocean: impact of the subsurface chlorophyll maximum on regional, seasonal and annual primary production estimates. *Biogeosciences* 10:1345–1399
- Arrigo KR, van Dijken GL (2011) Secular trends in Arctic Ocean net primary production. *J Geophys Res.* <https://doi.org/10.1029/2011JC007151>
- Arrigo KR, van Dijken GL (2015) Continued increases in Arctic Ocean primary production. *Prog Oceanogr* 136:60–70
- Arrigo KR, van Dijken GL, Pabi S (2008) Impact of a shrinking Arctic ice cover on marine primary production. *Geophys Res Lett.* <https://doi.org/10.1029/2008GL035028>
- Arrigo KR, Matrai PA, van Dijken GL (2011) Primary productivity in the Arctic Ocean: impact of complex optical properties and subsurface chlorophyll maxima on large-scale estimates. *J Geophys Res.* <https://doi.org/10.1029/2011JC007273>

- Bélangier S, Babin M, Tremblay JÉ (2013) Increasing cloudiness in Arctic damp the increase in phytoplankton primary production due to sea ice receding. *Biogeosciences* 10:4087–4101
- Bobrov UA, Savinov VM, Makarevich PR (1989) Chlorophyll and primary production. In: Ecology and bioresources of the Kara Sea. Kolsky scientific center, Apatity, pp 45–50 (in Russian)
- Brown ZW, Lowry KE, Palmer MA, van Dijken GL, Mills MM, Pickart RS, Arrigo KR (2015) Characterizing the subsurface chlorophyll *a* maximum in the Chukchi Sea and Canada Basin. *Deep Sea Res II* 118:88–104
- Cavaliere DJ, Parkinson CL (2012) Arctic sea ice variability and trends, 1979–2010. *Cryosphere* 6:881–889
- Cherkasheva A, Nöthig EM, Bauerfeind E, Melsheimer C, Bracher A (2013) From the chlorophyll-*a* in the surface layer to its vertical profile: a Greenland Sea relationship for satellite applications. *Ocean Sci* 9:431–445
- Comiso JC (2012) The rapid decline of multiyear ice cover. *J Clim*. <https://doi.org/10.1175/JCLI-D11-00113.1>
- Comiso JC, Parkinson CL, Gersten R, Stock L (2008) Accelerated decline in the Arctic sea ice cover. *Geophys Res Lett*. <https://doi.org/10.1029/2007GL031972>
- Cota GF, Pomeroy LR, Harrison WG, Jones EP, Peters F, Sheldon WM Jr, Weingartner TR (1996) Nutrients, primary production and microbial heterotrophy in the southeastern Chukchi Sea: Arctic summer nutrient depletion and heterotrophy. *Mar Ecol Progr Ser* 135:247–258
- Cullen JJ (2015) Subsurface chlorophyll maximum layers: enduring enigma or mystery solved? *Annu Rev Mar Sci* 7:207–239
- Demidov AB, Mosharov SA (2015) Vertical distribution of primary production and chlorophyll *a* in the Kara Sea. *Oceanology* 55:521–534
- Demidov AB, Mosharov SA, Makkaveev PN (2014) Patterns of the Kara Sea primary production in autumn: biotic and abiotic forcing of subsurface layer. *J Mar Sys* 132:130–149
- Demidov AB, Kopelevich OV, Mosharov SA, Sheberstov SV, Vazyulya SV (2017a) Modelling Kara Sea phytoplankton primary production: development and skill assessment of regional algorithms. *J Sea Res* 125:1–17
- Demidov AB, Sheberstov SV, Gagarin VI, Khlebopashev PV (2017b) Seasonal variation of the satellite-derived phytoplankton primary production in the Kara Sea. *Oceanology* 57:91–104
- Dittmar T, Kattner G (2003) The biogeochemistry of the river and shelf system of the Arctic Ocean: a review. *Mar Chem* 83:103–120
- Egge JK, Aksnes DL (1992) Silicate as regulating nutrient in phytoplankton competition. *Mar Ecol Progr Ser* 83:281–289
- Fisher TR, Peele ER, Ammerman JW, Harding LWJ (1992) Nutrient limitation of phytoplankton in Chesapeake Bay. *Mar Ecol Progr Ser* 82:51–63
- Fütterer DK, Galimov EM (2003) Siberian river run-off into the Kara Sea: characterization, quantification, variability and environmental significance - an introduction. In: Stein R, Fahl K, Fütterer DK, Galimov EM, Stepanets OV (eds) *Siberian river run-off in the Kara Sea*. Elsevier, Amsterdam, pp 1–8
- Gordeev VV, Kravchishina MD (2009) River flux of dissolved organic carbon (DOC) and particulate organic carbon (POC) to the Arctic Ocean: what are the consequences of the global changes? In: Nihoul JCJ, Kostianoy AG (eds) *Influence of climate change on the changing Arctic and Sub-Arctic conditions*. Springer, Dordrecht, pp 145–160
- Gordeev VV, Martin JM, Sidorov IS, Sidorova MV (1996) A reassessment of the Eurasian river input of water, sediment, major elements and nutrients to the Arctic Ocean. *Am J Sci* 296:664–691
- Grasshoff K, Kremling K, Ehrhardt M (1999) *Methods of seawater analysis*, 3rd edn. Wiley, New York
- Hansen HP, Koroleff F (1999) Determination of nutrients. In: Grasshoff K, Kremling K, Ehrhardt M (eds) *Methods of seawater analysis*, 3rd edn. Wiley, New York, pp 149–228
- Hanzlick D, Aagaard K (1980) Freshwater and Atlantic water in the Kara Sea. *J Geophys Res* 85:4937–4942
- Hill VJ, Cota GF (2005) Spatial patterns of primary production on the shelf, slope and basin of the Western Arctic in 2002. *Deep Sea Res II* 57:3344–3354
- Hill VJ, Zimmerman RC (2010) Estimates of primary production by remote sensing in the Arctic Ocean: assessment of accuracy with passive and active sensors. *Deep Sea Res I* 57:1243–1254
- Hill VJ, Matrai PA, Olson E, Suttles S, Steele M, Codispoti LA, Zimmerman RC (2013) Synthesis of integrated primary production in the Arctic Ocean: II. In situ and remotely sensed estimates. *Prog Oceanogr* 110:107–125
- Holmes RM, Peterson BJ, Gordeev VV, Zhulidov AV, Meybeck M, Lammers RB, Vörösmarty CJ (2000) Flux of nutrients from Russian rivers to the Arctic Ocean: can we establish a baseline against which to judge future changes? *Water Resour Res* 36:2309–2320
- Holmes RM, McClelland JW, Peterson BJ, Tank SE, Bulygina E, Eglington TI, Gordeev VV, Gurtovaya TY, Raymond PA, Repeta DJ, Staples R, Striegl RG, Zhulidov AV, Zimov SA (2012) Seasonal and annual fluxes of nutrients and organic matter from large rivers to the Arctic Ocean and surrounding seas. *Estuaries Coasts* 35:369–382
- Holm-Hansen O, Riemann B (1978) Chlorophyll *a* determination: improvements in methodology. *Oikos* 30:438–447
- Holm-Hansen O, Lorenzen CJ, Holmes RW, Strickland JDH (1965) Fluorometric determination of chlorophyll. *J Cons Perm Int Explor Mer* 30:3–15
- Kubryakov A, Stanichny S, Zatsepin A (2016) River plume dynamics in the Kara Sea from altimetry-based lagrangian model, satellite salinity and chlorophyll data. *Remote Sens Environ* 176:177–187
- Kwok R, Cunningham GF, Wensnahan M, Rigor I, Zwally HJ, Yi D (2009) Thinning and volume loss of Arctic sea ice: 2003–2008. *J Geophys Res*. <https://doi.org/10.1029/2009JC005312>
- Le Fouest V, Babin M, Tremblay JÉ (2013) The fate of riverine nutrients on Arctic shelves. *Biogeosciences* 10:3661–3677
- Lee SH, Whitley TE (2005) Primary and new production in the deep Canada Basin during summer 2002. *Polar Biol* 28:190–197
- Lee YJ, Matrai PA, Friedrichs MAM, Saba VS, Antoine D, Ardyna M, Asanuma I, Babin M, Bélangier S, Benoit-Gagné M, Devred E, Fernández-Méndez M, Gentili B, Hirawake T, Kang Sung-Ho, Kameda T, Katlein C, Lee SH, Lee Z, Mélin F, Scardi M, Smyth TJ, Tang S, Turpie KR, Waters KJ, Westberry TK (2015) An assessment of phytoplankton primary productivity in the Arctic Ocean from satellite ocean color/in situ chlorophyll-*a* based models. *J Geophys Res* 120:6508–6541
- Leu E, Søreide JE, Hessen DO, Falk-Petersen S, Berge J (2011) Consequences of changing sea-ice cover for primary and secondary producers in the European Arctic shelf seas: timing, quantity, and quality. *Prog Oceanogr* 90:18–32
- Makkaveev PN (1998) The total alkalinity in the anoxic waters of the Black Sea and in sea-river mixture zones. In: Annex V (ed) *Proceedings of 7th Session of Intergovernmental Oceanographic Commission. Joint IOC-JGOFS CO<sub>2</sub> Advisory Panel Meeting, UNESCO*
- Martin J, Tremblay JÉ, Gagnon J, Tremblay G, Lapoussié A, Jose C, Poulin M, Gosselin M, Gratton Y, Michel C (2010) Prevalence, structure and properties of subsurface chlorophyll maxima in Canadian Arctic waters. *Mar Ecol Progr Ser* 412:69–84
- Martin J, Tremblay JÉ, Price NM (2012) Nutritive and photosynthetic ecology of subsurface chlorophyll maxima in Canadian Arctic waters. *Biogeosciences* 9:5353–5371

- Matrai PA, Olson E, Suttles S, Hill V, Codispoti LA, Light B, Steele M (2013) Synthesis of primary production in the Arctic Ocean: I. Surface waters, 1954–2007. *Prog Oceanogr* 110:93–106
- Millero FJ (1995) Thermodynamics of the carbon dioxide system in oceans. *Geochim Cosmochim Acta* 59:661–677
- Mosharov SA (2010) Distribution of the primary production and chlorophyll *a* in the Kara Sea in September of 2007. *Oceanology* 50:885–893
- Mosharov SA, Demidov AB, Simakova UV (2016) Peculiarities of the primary production process in the Kara Sea at the end of the vegetation season. *Oceanology* 56:84–94
- Opsahl S, Benner R, Amon RW (1999) Major flux of terrigenous dissolved organic matter through the Arctic Ocean. *Limnol Oceanogr* 44:2017–2023
- Pabi S, van Dijken GL, Arrigo KR (2008) Primary production in the Arctic Ocean, 1998–2006. *J Geophys Res*. <https://doi.org/10.1029/2007/JC004578>
- Petrenko D, Pozdnyakov D, Johannessen J, Counillon F, Sychov V (2013) Satellite-derived multi-year trend in primary production in the Arctic Ocean. *Int J Remote Sens* 34:3903–3937
- Pivovarov S, Schlitzer R, Novikhin A (2003) River run-off influence on the water mass formation in the Kara Sea. In: Stein R, Fahl K, Fütterer DK, Galimov EM, Stepanets OV (eds) *Siberian river run-off in the Kara Sea*. Elsevier, Amsterdam, pp 9–25
- Rachold V, Eicken H, Gordeev VV, Grigoriev MN, Hubberten HW, Lisitzin AP, Shevchenko VP, Schirrmeister L (2004) Modern terrigenous organic carbon input to the Arctic Ocean. In: Stein R, Macdonald RW (eds) *The organic carbon cycle in the Arctic Ocean*. Springer-Verlag, Berlin, pp 33–56
- Ryther JH, Yentsch CS (1957) The estimation of phytoplankton production in the ocean from chlorophyll and light data. *Limnol Oceanogr* 2:281–286
- Sakshaug E (2004) Primary and secondary production in the Arctic Seas. In: Stein R, Macdonald RW (eds) *The organic carbon cycle in the Arctic Ocean*. Springer, Berlin, pp 57–81
- Stemann Nielsen E (1952) The use of radioactive carbon ( $C^{14}$ ) for measuring organic production in the sea. *J Cons Perm Int Explor Mer* 18:117–140
- Stein R (2000) Circum Arctic river discharge and its geological record. *Int J Earth Sci* 89:447–449
- Stroeve J, Holland M, Meier W, Scambos T, Serreze M (2007) Arctic sea ice decline: faster than forecast. *Geophys Res Lett*. <https://doi.org/10.1029/2007GL029703>
- Stroeve J, Kattsov V, Barrett A, Serreze M, Pavlova T, Holland M, Meier WN (2012a) Trends in Arctic sea ice extent from CMIP5, CMIP3 and observations. *Geophys Res Lett*. <https://doi.org/10.1029/2012GL052676>
- Stroeve J, Serreze M, Holland M, Kay J, Malanik J, Barrett A (2012b) The Arctic's rapidly shrinking sea ice cover: a research synthesis. *Clim Change* 110:1005–1027
- Timmermans ML, Cole S, Toole J (2012) Horizontal density structure and restratification of the Arctic Ocean surface layer. *J Phys Oceanogr* 42:659–668
- Tremblay JÉ, Gagnon J (2009) The effect of irradiance and nutrient supply on the productivity of Arctic waters: a perspective on climate change. In: Nihpul JCJ, Kostianoy AG (eds) *Influence of climate change on the changing Arctic and Sub-Arctic condition*. Springer, New York, pp 73–94
- Tremblay JÉ, Michel C, Hobson KA (2006) Bloom dynamics in early opening waters of the Arctic Ocean. *Limnol Oceanogr* 51:900–912
- Uitz J, Claustre H, Morel A, Hooker SB (2006) Vertical distribution of phytoplankton communities in open ocean: an assessment on surface chlorophyll. *J Geophys Res* 111:C08005. <https://doi.org/10.1029/2005JC003207>
- UNESCO (1983) *IOC manuals and guides 12. Chemical methods for use in marine environment monitoring*
- Vancoppenolle M, Bopp L, Madec G, Dunne J, Ilyina T, Halloran PR, Steiner N (2013) Future Arctic Ocean primary productivity from CMIP5 simulations: uncertain outcome, but consistent mechanisms. *Glob Biogeochem Cycle*. <https://doi.org/10.1002/gbc.20055>
- Vedernikov VI, Demidov AB, Sud'bin AI (1995) Primary production and chlorophyll in the Kara Sea in September 1993. *Oceanology* 34:630–640
- Vetrov AA, Romankevich EA (2004) *Carbon cycle in the Russian Arctic seas*. Springer, Berlin
- Zatsepin AG, Zavialov PO, Kremenetskiy VV, Poyarkov SG, Soloviev DM (2010) The upper desalinated layer in the Kara Sea. *Oceanology* 50:658–668
- Zatsepin AG, Zavialov PO, Baranov VI, Kremenetskiy VV, Nedospasov AA, Poyarkov SG, Ocherednik VV (2017) On the mechanism of wind-induced transformation of a river runoff water lens in the Kara Sea. *Oceanology* 57:1–7
- Zhai L, Gudmundsson K, Miller P, Peng W, Guðfinnsson H, Debes H, Hátún H, White GN, Hernández Walls R, Sathyendranath S, Platt T (2012) Phytoplankton phenology and production around Iceland and Faroes. *Cont Shelf Res* 37:15–25
- Zhang J, Spitz YH, Steele M, Ashjian C, Campbell R, Berline L, Matrai P (2010) Modeling the impact of declining sea ice on the Arctic marine planktonic ecosystem. *J Geophys Res*. <https://doi.org/10.1029/2009/JC005387>